Nature of Clay–Humic Complexes in an Agricultural Soil: II. Scanning Electron Microscopy Analysis

David Laird*

ABSTRACT

The most stable forms of organic matter in soils are the clay–humic complexes. An understanding of mechanisms and processes influencing the formation of clay–humic complexes may facilitate development of agricultural management systems that increase the long-term sequestration of C in soils and improve soil quality. The specific objective of this study was to visualize associations between humic substances and clay minerals separated from a typical agricultural soil. The soil sample used in this study was from the Ap horizon of a Webster (fine-loamy, mixed, superactive, mesic Typic Endoaquoll) soil located near Waseca, MN. The whole soil clay fraction (<2 μm particle-size fraction) was separated by a relatively mild sedimentation technique, and coarse, medium, and fine clay fractions (0.2–2.0, 0.02–0.2, and <0.02 μm size fractions, respectively) were separated from a portion of the whole clay sample by an aggressive sonication-centrifugation technique. All samples were Ca-saturated, dialyzed, and freeze-dried. The samples were analyzed by scanning electron microscopy to obtain images of clay–humic complexes and energy dispersive x-ray analysis to obtain maps of elemental distributions. Two distinct types of clay-associated humic substances were identified. The first type exists as diffuse filamentous films that cover basal surfaces of 2:1 phyllosilicates in the medium and fine clay fractions. The second type exists as discrete particles of high-density metal–humic substance complexes in the coarse clay fraction.

M UCH CURRENT RESEARCH is focused on documenting management influences on sequestration of C in soils (Lal et al., 1997). Recent estimates (Bruce et al., 1999) suggest that with prudent management agricultural soils in the USA and Canada could gain 1.1×10^{15} g of C over the next two decades, and thereby contribute about 15% of the net reductions in C emissions needed to bring the USA and Canada into compliance with the Kyoto Protocols (United Nations, 1997) regulating atmospheric levels of greenhouse gases. Furthermore, increasing the amount of organic matter in soils increases the ability of soil to supply water, air, and nutrients to growing plants and thus has a positive effect on soil quality.

Most management recommendations for increasing levels of organic matter in soils are focused on increasing the amount of plant residue returned to the soil and decreasing the intensity of tillage. While increased residue additions certainly increases short-term storage of C in soils, the long-term impact of increased residue additions on C sequestration is questionable. Fresh residues decompose rapidly in soil environments and typically over half of the C in fresh residue is mineralized to CO_2 within a few weeks or months (Ajwa and Tabatabai, 1994). By contrast, the C in recalcitrant clay–humic com-

plexes has mean residence times in soils of 500 to 3000 yr (Oades, 1988, 1989; Stevenson, 1994). Thus, the long-term impact of soil and residue management systems on C sequestration depends on whether the management systems encourage or discourage the formation of highly recalcitrant clay–humic complexes.

The goal of our research was to develop an understanding of the influence of clay mineralogy on the formation and stabilization of humic substances in soils. It is anticipated that increased understanding of the mechanisms and processes that cause formation of recalcitrant clay–humic complexes in soils will facilitate development of soil and residue management systems that optimize both C sequestration and soil quality enhancement. The first manuscript of this series (Laird et al., 2001) presents evidence relating the mineralogy of various clay fractions isolated from a Webster soil and the chemical, biochemical, and spectroscopic characteristics of the associated humic substances. The results indicate that humic substances are intimately associated with soil clay minerals and that humic substances associated with different clay fractions have unique chemical, biochemical, and functional properties. The specific objective of the present study is to visualize the nature of the associations between humic substances and clay minerals in the clay fractions isolated from the Webster soil.

The mineralogy of the Webster soil clay has been studied in great detail (Laird et al., 1991; Laird and Nater, 1993). Coarse clay separates are dominated by quartz with lesser amounts of 10Å-illite, kaolinite, and feldspars. Fine clay separates contain smectite and a low-charged interstratified phase. The smectite is a high Fe montmorillonite with a moderate layer charge [0.482 ($-$) per half unit cell] and 47% tetrahedral charge. The low-charged interstratified phase consists of randomly interstratified 10 and 15 Å 2:1 phyllosilicate layers with a layer charge of 0.473 ($-$) per half unit cell and 87% tetrahedral charge (Laird et al., 1991). Although, the low-charged interstratified phase can not be classified using current nomenclature guidelines (Bailey et al., 1982), it has unofficially been referred to as *protoillite* (Laird and Dowdy, 1994) and that convention will be followed hereafter in the present manuscript.

MATERIALS AND METHODS

The soil sample used in this study was collected from the Ap horizon (0–5 cm) of a Webster pedon located in an agricultural field on the University of Minnesota Southern Agricultural Experiment Station, near Waseca, MN. Details of sample preparation and fractionation have been described previously

Abbreviations: MAS-NMR, magic angle spinning-nuclear magnetic resonance spectroscopy; SEM, scanning electron microscopy; XRD, x-ray diffraction.

(Laird et al., 2001). Briefly, the soil was mechanically dispersed in distilled water and a bulk sample of the soil clay (<2 μm particle-size fraction) was separated by sedimentation and air dried. A portion of the <2 μm particle-size fraction was saved as the whole clay fraction and another portion was subjected to seven cycles of dispersion by sonication, centrifugation, and decantation to separate the coarse (0.2–2.0 μm), medium (0.02–0.2 μm), and fine (<0.02 μm) clay fractions.

Mineralogy of the clay fractions was analyzed using both chemical analysis and x-ray diffraction (XRD). The quantity and nature of the organic matter associated with each clay fraction were analyzed using chemical, biochemical, and spectroscopic techniques. Details of XRD, chemical, biochemical, and spectroscopic analyses of the various soil clay fractions along with results are given in the first manuscript of the series (Laird et al., 2001).

In this study, the untreated and H_2O_2-treated samples were analyzed by scanning electron microscopy (SEM) using a JEOL[1] (JEOL U.S.A., Peabody, MA) JSM-5800LV SEM. The samples were prepared for the SEM analysis by first sonicating 5 μg of clay for 30 s in 10 mL of H_2O and then transferring 50 μL of suspension to Al-SEM studs covered with Al foil. The samples were dried in a desiccator, sputter coated with Au-Pd, and then analyzed at 10 kV. Stereo pairs were obtained by taking one image of a given area and then tilting the sample stage 10° with respect to the detector and then taking a second image of the same region.

Humic substances in the coarse clay fraction were labeled with Cu and then analyzed using elemental mapping. To do so, a sample of the coarse clay fraction was equilibrated for 24 h at room temperature with 0.001 M $CuCl_2$ plus 0.01 M $CaCl_2$. Following the equilibration, the supernatant was separated by centrifugation and discarded. To remove readily exchangeable Cu, the sample was equilibrated for an additional 25 h with 0.01 M $CaCl_2$, centrifuged, and the supernatant was discarded. Elemental mapping was done using a Quantum Kevex energy-dispersive detector (Thermo–Noran, Madison, WI) equipped with a Be window positioned 20 mm above the sample. The SEM was operated at 25 kV and the final aperture was removed to enhance signal collection.

RESULTS AND DISCUSSION

Soil organic matter includes both clay–humic complexes and biological materials. The term *biological materials* refers to living organisms and the partly decomposed remains of plant, fungal, and microbial tissues. Biological materials are easily recognized in scanning electron micrographs because they retain cell wall or other structural features unique to biological tissues. For this study, four different specimens from each of the four clay fractions were analyzed by SEM during ~20 h of beam time, and a total of 125 micrographs were taken. While thousands of clay–humic complexes and individual mineral grains were observed, only two particles were clearly identified as biological materials. Thus it is apparent that the fractionation procedure used in this study was highly effective for separating biological materials from the clay–humic complexes.

The whole clay fraction contains 63.2 g C kg^{-1}, 5.0 g N kg^{-1}, and in decreasing order of abundance smectite, protoillite, quartz, kaolinite, 10Å-illite, and feldspars (Laird et al., 2001). Scanning electron micrographs of the whole clay fraction are presented in Fig. 1. Both large aggregated structures (5–20 μm) and discrete particles (0.5–2 μm) are evident in the SEMs of the whole clay. The aggregated structures are roughly equal dimensional but have many surface irregularities. A few angular mineral grains can be seen either sitting on, or protruding from, the aggregated structures; however, most surfaces have a diffuse-porous appearance suggesting that they are covered with humic materials. Scanning electron micrographs of the H_2O_2-treated whole clay fraction (data not shown) revealed numerous individual mineral grains, a few small aggregated structures, but no large aggregated structures. Because of their morphology, the known chemical and mineralogical composition of the whole clay fraction, and the fact that a minimum amount of mechanical energy was used to separate the whole clay fraction from the soil; the large aggregated structures are believed to be intact microaggregates that are held together by humic substances. These microaggregates probably existed in the soil at the time of sampling as components of larger soil structural units.

The sedimentation technique used to collect the whole clay fraction was designed, based on Stokes law, to collect spherical particles with a density of 2.65 g cm^{-3} and a diameter of <2 μm. Obviously, many of the microaggregates in the whole clay fraction (Fig. 1) are significantly larger than 2 μm. Assuming the largest of the microaggregates are 20-μm spheres, then Stokes law may be solved to estimated their density as 1.02 g cm^{-3}. Such a low density is consistent with high levels of humic material and substantial internal porosity.

The SEMs of the whole clay fraction revealed numerous small discrete particles scattered among the microaggregates. High resolution SEMs (Fig. 1C) revealed three types of discrete particles. The first particle type are small platy mineral particles with diffuse surfaces. These platy particles are believed to be 2:1 phyllosilicates with surface coatings of humic substances. The second particle type is composed of roughly equal dimensional particles with rounded edges and smooth surfaces. These rounded particles are believed to be quartz and feldspar grains with either very thin or no surface coatings of humic substances. The third particle type is composed of roughly equal dimensional particles with nodular surfaces. The nature of the nodular particles is not immediately apparent, but the nodular particles are obviously not phyllosilicates nor are they discrete quartz or feldspar grains. Therefore, by process of elimination, the nodular particles must be either metal-oxyhydroxy minerals or discrete particles of humic substances.

The coarse, medium, and fine clay fractions were separated from the whole clay fraction using an aggressive procedure that included seven cycles of resuspension, dispersion by sonication, centrifugation, and decantation. The procedure destroyed most if not all of the soil microaggregates and successfully dispersed the individ-

ual mineral grains allowing separation of the coarse, medium, and fine clay fractions which are dominated by quartz, protoillite, and smectite, respectively (Laird et al., 2001). The coarse, medium, and fine clay fractions contain similar amounts of organic C; however, chemical, biochemical, and spectroscopic analyses revealed substantial differences in the nature of the humic substances associated with these mineralogically significant clay fractions (Laird et al., 2001). The C/N ratios of humic substances associated with the coarse, medium, and fine clay fractions are 17, 10, and 10, respectively. The coarse clay fraction has stronger carboxyl and O-alkyl ^{13}C-NMR peaks and lower levels of extractable amino acids, fatty acids, monosaccharides, and amino sugars than the fine clay fraction.

Chemical and XRD analyses (Laird et al., 2001) indicate that the fine clay fraction contains 51.7 g C kg^{-1} clay and is dominated by smectite (82% w/w) with lesser amounts of protoillite (18% w/w). The SEM analysis of the fine clay fraction (Fig. 2) revealed numerous large particles (10–50 µm) and only a few small particles (0.5–2 µm). The size of most of the large particles is significantly greater than that of the microaggregates observed in the whole clay fraction (Fig. 1). Thus it is obvious that the large particles in the fine clay fraction did not exist in the whole clay fraction but were formed during sample preparation probably when excess NaCl was added to the highly dispersed fine clay suspension to cause flocculation. Subsequent treatments, including Ca-saturation, dialysis, freeze-drying, resuspension, and drying on the SEM studs, may also have affected the size and appearance of the large particles in the fine clay fraction.

In high resolution micrographs (Fig. 3A), surfaces of the large smectite particles exhibit prominent light colored ropy features and diffuse dark blotchy regions between the ropy features. Surfaces of the H$_2$O$_2$-treated particles (Fig. 3B) also exhibit the prominent ropy features but have a more uniform coloration in the dark regions between the ropy structures. Subtle differences in the shape and distribution of the blotchy features between the left and right half of the stereo pair (Fig. 3A) appear as diffuse structures protruding above surfaces of the untreated particles when viewed in 3D. By contrast, surfaces of the H$_2$O$_2$-treated particles (Fig. 3B) have a smoother appearance. Appreciation of the differences between the surface textures of the H$_2$O$_2$-treated and untreated particles requires careful study of the micrographs shown in Fig. 3A and 3B. The blotchy structures observed in Fig. 3A appear to be a loosely woven network of filamentous material enmeshing basal surfaces of the smectite particles. The prominent ropy structures are most likely wrinkles of the surficial smectite layer(s) that are protruding through the diffuse surface films.

Many of the small particles in the fine clay fraction appeared to be extensively wrinkled (crumpled) smectite layers, while others appeared to be relatively thick stacks of rigid 2:1 phyllosilicate layers, probably protoillite (Fig. 2C). Fundamental particles of protoillite consist of two 2:1 phyllosilicate layers glued together with dehydrated K and therefore should be more rigid than
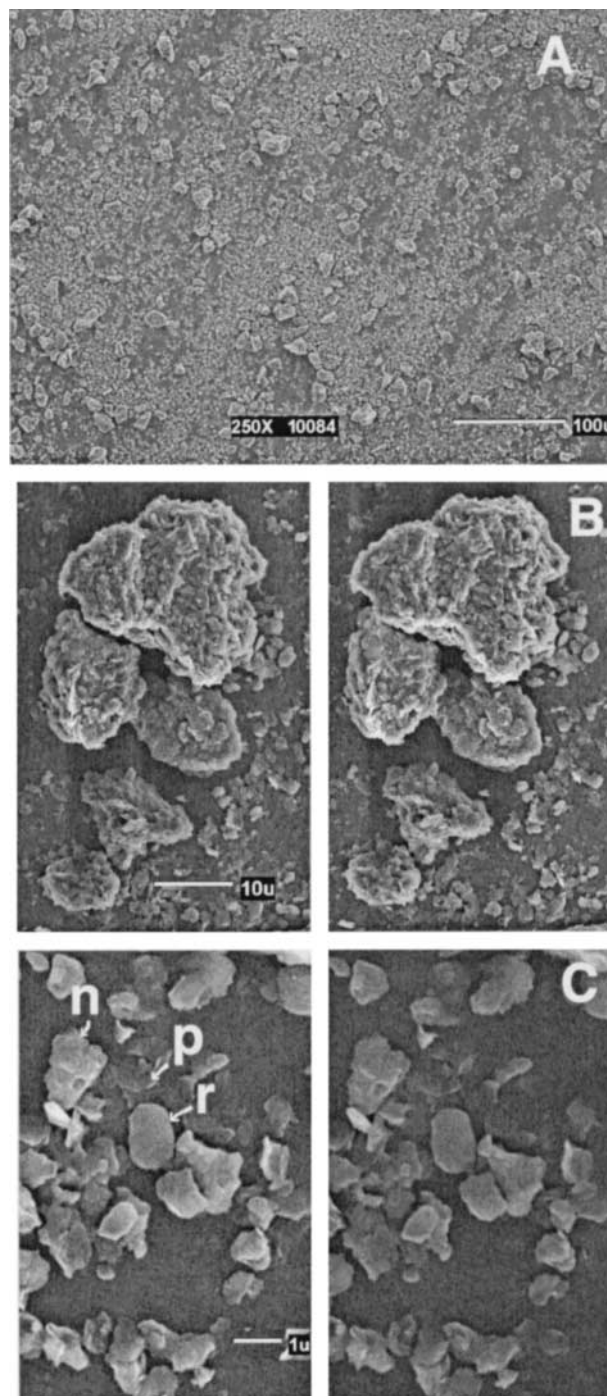

Fig. 1. Scanning electron micrographs of the whole clay fraction from the Webster soil; (A) low magnification scanning electron microscopy (SEM) illustrating large (5–20 µm) soil microaggregates and small (0.5–2 µm) discrete particles, (B) medium magnification SEM stereo pair of a typical soil microaggregate, and (C) high magnification SEM stereo pair illustrating small particles with platy (p), rounded (r), and nodular (n) morphologies.

fundamental smectite particles which consist of only one 2:1 phyllosilicate layer (Laird et al., 1991; Laird and Nater, 1993). Many surfaces of the small particles in the fine clay fraction are also covered with diffuse filamentous material.

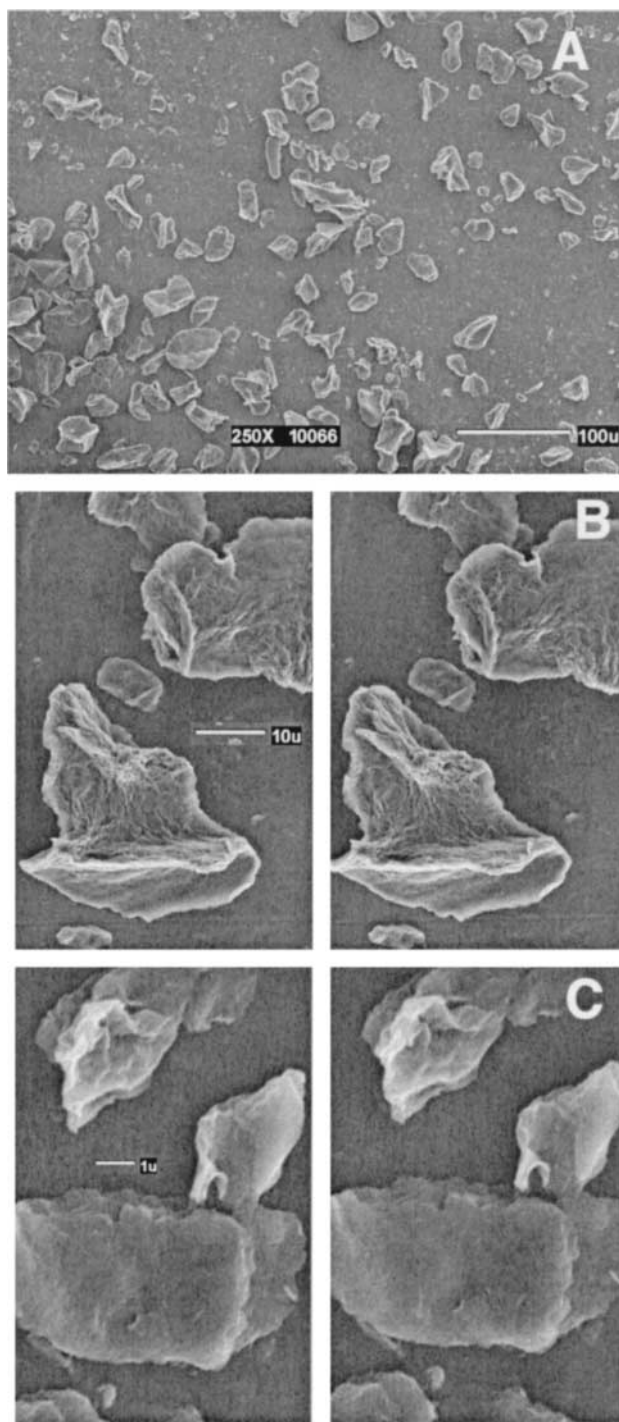The amount of organic C (51.7 g C kg^{-1} clay) in the

Fig. 2. Scanning electron micrographs of the fine clay fraction from the Webster soil; (A) low magnification scanning electron microscopy (SEM) illustrating numerous large (10–50 μm) and only a few small (0.5–5 μm) particles, (B) medium magnification SEM stereo pair of typical large smectite particles, and (C) high magnification SEM stereo pair of thin crumpled and thicker more rigid platy particles.

Fig. 3. High resolution stereo scanning electron micrographs of particle surfaces from the untreated (A) and H$_2$O$_2$-treated (B) fine clay fraction of the Webster soil. The prominent ropy structures are believed to be wrinkles in the surficial smectite layers. Subtle blotchy features between the ropy structures seen in A but not seen in B are believed to be diffuse filamentous coatings of humic materials. The volcano was probably caused by a gas bubble that burst through the top smectite layer when the sample was evacuated.

fine clay fraction is so large that the organic phase should be readily apparent in the SEMs. However, all of the particles observed in the SEMs of the fine clay fraction exhibit platy or sheet-like morphologies, consistent with smectite and protoillite, the only mineral phases 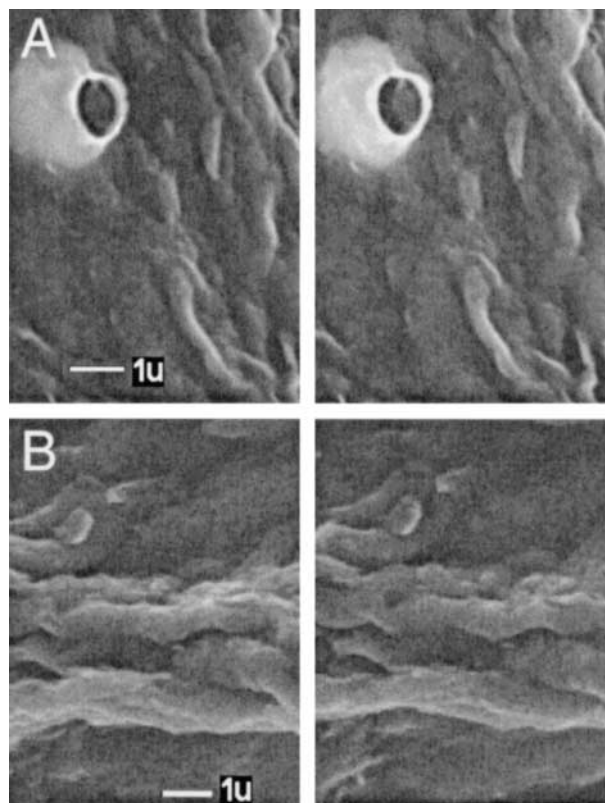identified in the sample by XRD. Humic substances have never been reported to assume a platy or sheet-like morphology. On the other hand, humic materials are known to be strongly retained as diffuse films on external surfaces of smectites and other phyllosilicates (Stevenson, 1994; Schnitzer, 1986; Oades, 1989). Thus, it is concluded that the organic C is concentrated in the diffuse filamentous coatings observed on surfaces of the mineral particles in the fine clay fraction. This does not preclude the possibility that inorganic materials also contribute to the observed diffuse films either as complexes with the humic substances or as a discrete phase.

Chemical and XRD analyses of the medium clay fraction indicate a C content of 67.2 g C kg^{-1} clay and three mineral phases, protoillite (70% w/w), smectite (25% w/w), and kaolinite (5% w/w). The SEMs of the medium clay fraction (Fig. 4) reveal a bimodal particle-size distribution that includes large (5–20 μm) and small (0.1–2 μm) particles. The large particles in the medium clay fraction are approximately the same size and shape as the soil microaggregates observed in the whole clay fraction (Fig. 1). However, it is unlikely that the large particles in the medium clay fraction are soil microaggregates that remained intact through the fractionation procedure. Mineralogical differences between the whole clay and medium clay fractions suggests that the large

particles were formed during sample preparation when the dispersed medium clay suspension was flocculated. Surfaces of the large particles in the medium clay fraction are difficult to observe because the large particles are covered with numerous small particles. Most of the small particles have a platy morphology, many appear to be roughly circular plates while others appear to be crumpled sheets. The small circular plates maybe protoillite while the crumpled sheets are more likely smectite. Surfaces of all of the particles in the medium clay fraction appear covered with diffuse filamentous humic films similar to those observed covering surfaces of smectite particles in the fine clay fraction.

X-ray diffraction and chemical analyses (Laird et al., 2001) indicated that the coarse clay is dominated by quartz with lesser amounts of kaolinite, 10Å-illite, and feldspars. The coarse- clay fraction contains a very large amount of organic C, 69.8 g C kg^{-1} clay. If the organic phase has a density of 1 g cm^{-3} then it should be about 27% of the sample volume (assuming organic matter % = organic C % $\times$ 1.7 and assuming a density of 2.65 g cm^{-3} for all mineral particles). If the organic phase were more or less uniformly distributed over all particle surfaces it should be plainly visible as very thick diffuse films. However, there is no evidence of thick surface films (Fig. 5); surfaces of most particles appear smooth, many particles exhibit sharp corners and angular edges which would be obscured by thick organic films, and thick organic films would cause the particles to flocculate whereas the particles in the coarse clay fraction are obviously individual grains (Fig. 5). Therefore, the organic phase must be both condensed and concentrated in discrete particles.

Four distinct particle morphologies are evident in the SEMs of the coarse clay fraction (Fig. 5); including rounded particles with smooth surfaces, angular particles with smooth surfaces, platy particles with smooth surfaces, and nodular particles with rough or irregular surfaces. The platy particles are clearly phyllosilicates. The smooth surfaces of the rounded and angular particles suggests that they are crystalline. Indeed, most of the rounded and angular particles must be quartz, as quartz is the most abundant mineral phase in the coarse clay fraction. Thus by process of elimination the organic phase is probably concentrated in the nodular particles. Some of the nodular particles are also likely to be discrete metal-oxyhydroxide minerals.

The coarse clay was the residue in the bottom of the centrifuge tubes after seven sequential dispersion-centrifugation-decantation cycles. By repeating the process seven times virtually all particles <0.2 μm and virtually all particles in the 0.2 to 2.0-μm size range with densities significantly <2.65 g cm^{-3} were removed from the coarse clay fraction (the supernatant for the last cycle was virtually clear). The SEM analysis revealed that virtually all of the particles in the coarse clay fraction (Fig. 5) are individual roughly equal dimensional grains (grains that should behave like spheres in a centrifugal field) within the anticipated 0.2 to 2.0 μm size range. Furthermore, the dominant mineral phase in the coarse clay fraction is quartz (Laird et al., 2001) which
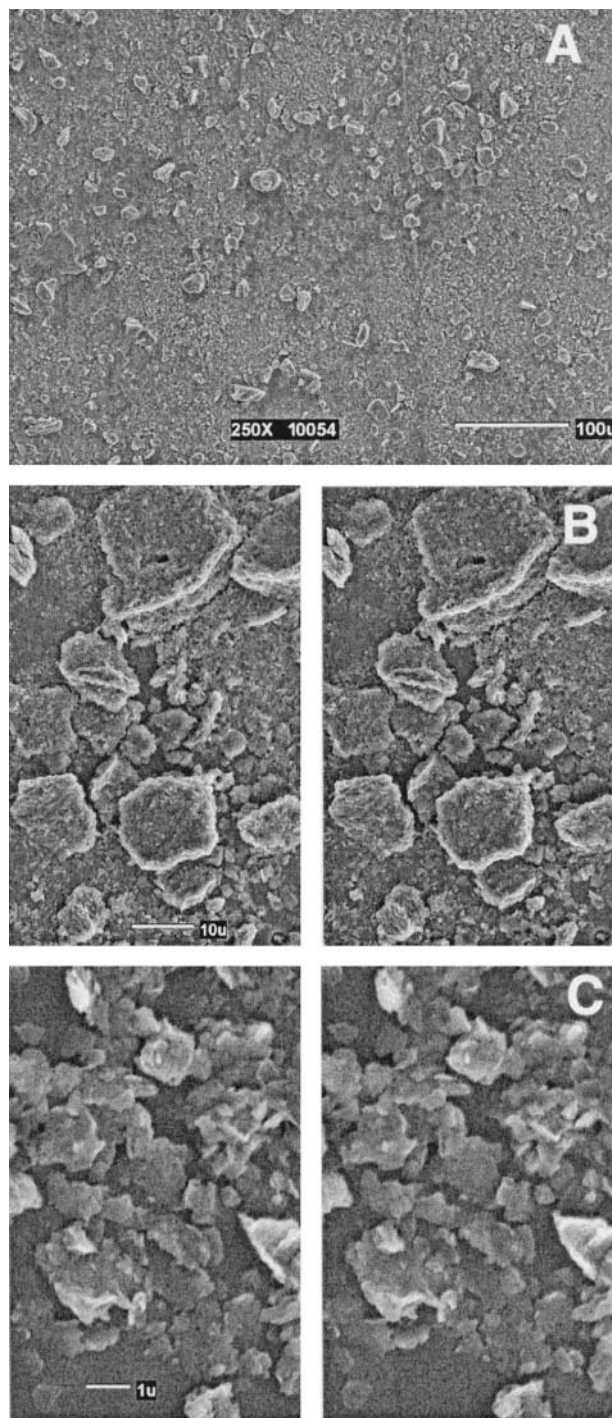

Fig. 4. Scanning electron micrographs of the medium clay fraction from the Webster soil; (A) low magnification scanning electron microscopy (SEM) illustrating numerous large (5–20 μm) and small (1–2 μm) particles, (B) medium magnification SEM stereo pair illustrating typical large particles covered with small particles, and (C) high magnification SEM stereo pair of small protoillite and smectite particles.

has a densities of 2.65 g cm^{-3}. Therefore, it is concluded that the density of discrete organic particles present in the coarse clay fraction must be about 2.65 g cm^{-3}. This conclusion is counterintuitive, as most organic materials have densities <1 g cm^{-3}. The conclusion is unavoidable, however, given knowledge of how the coarse clay frac-
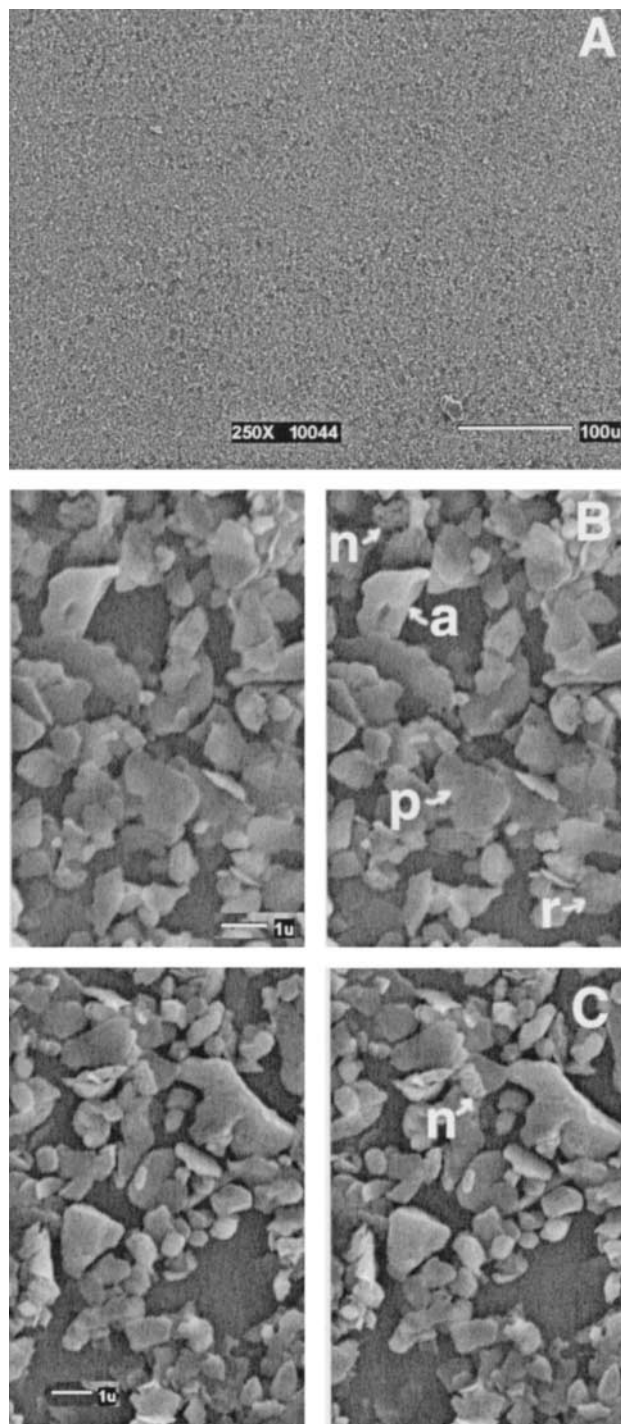
Fig. 5. Scanning electron micrographs of the coarse clay fraction from the Webster soil; (A) low magnification scanning electron microscopy (SEM) illustrating numerous small (0.2–2 μm) discrete particles and only a few small (1–3 μm) aggregates, (B) and (C) high magnification SEM stereo pairs illustrating platy (p), rounded (r), angular (a), and nodular (n) morphologies of the small discrete particles. Most of the surfaces of the platy and rounded particles appear smooth indicating that these particles are either uncoated or have very thin coatings of humic substances.
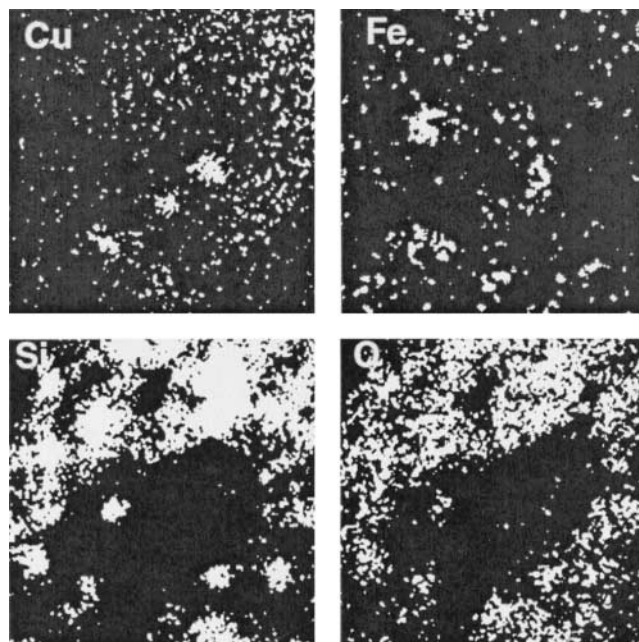

Fig. 6. Energy dispersive x-ray adsorption maps of elemental distributions in small discrete particles from the coarse clay fraction from the Webster soil. Three discrete particles with high Cu concentrations (assumed to be discrete humic particles) also have high Fe but low Si and O levels. The elemental maps are ~10 μm on each side. The elemental maps were electronically filtered to reduce noise and enhance contrast.

it is hypothesized that the discrete organic particles in the coarse clay fraction contain a relatively large amount of heavier elements (e.g., metals).

The hypothesis that the coarse clay fraction contains discrete high density organic particles containing high levels of metals was tested by using energy dispersive x-ray analysis to map distributions of Cu, Fe, Si, and O in particles of the coarse clay fraction (Fig. 6). The sample had been pretreated with Cu because previous work (Wu et al., 1999) indicates that humic substances associated with the coarse clay fraction have a high affinity for Cu, and thus the Cu distribution should indicate the C distribution. Evident in Fig. 6 are three hot spots for Cu. The Cu hot spots have elevated Fe but low Si and O levels. Thus, assuming the Cu distribution is an accurate indication of the C distribution, then the results of the elemental mapping support the hypothesis that C and Fe (and presumably other metals) are concentrated in discrete high density particles. The elemental mapping also provides evidence for a separate Fe-rich phase with low C (probably one of the Fe-oxyhydroxide minerals). Unfortunately, the accompanying image of the mapped area is of low quality because the SEM was optimized for elemental analysis rather than image analysis. Thus, it was not possible to determine whether the particles with the high Cu levels also exhibit the nodular surface morphology.

CONCLUSIONS

Scanning electron microscopy in conjunction with XRD, chemical, biochemical, and spectroscopic analy-

tion was prepared, SEMs that show nothing but discrete particles within the anticipated size range, and a measured organic C content of nearly 7% by weight. To explain the apparent high density of the organic phase,

ses have revealed the existence of two distinct types of clay-associated humic substances in the Webster soil. The first type of humic substance exists as a diffuse filamentous film that covers surfaces of smectite and protoillite particles in the medium and fine clay fractions. The first type has a low C/N ratio (10), high levels of extractable biomolecules (primarily amino acids and fatty acids), and relatively strong ^{13}C MAS-NMR peaks in the aliphatic region. The second type of humic substance exists as discrete high-density metal-humic complexes. The second type has a higher C/N ratio (17), lower levels of extractable biomolecules, and produces relatively stronger ^{13}C MAS-NMR peaks in the carboxyl, O-alkyl, and alkene-aromatic regions. Future investigations will focus on the genesis, lability, and relative ages of the various clay–humic complexes in an effort to relate the findings to C sequestration and soil quality.

REFERENCES

Ajwa, H.A., and M.A. Tabatabai. 1994. Decomposition of different organic materials in soils. Biol. Fertil. Soils 18:175–182.

Bailey, S.W., G.W. Brindley, H. Kodama, and R.T. Martin. 1982. Report of the Clay Minerals Society Nomenclature Committee for 1980 and 1981: Nomenclature for regular interstratifications. Clays Clay Miner. 30:76–78.

Bruce, J.P., M. Frome, E. Haites, H. Janzen, R. Lal, and K. Paustian. 1999. Carbon sequestration in soils. J. Soil Water Conserv. 54:382–386.

Laird, D.A., P. Barak, E.A. Nater, and R.H. Dowdy. 1991. Chemistry of smectitic and illitic phases in interstratified soil smectite. Soil Sci. Soc. Am. J. 55:1499–1504.

Laird, D.A., and E.A. Nater. 1993. Nature of the illitic phase associated with randomly interstratified smectite/illite in soils. Clays Clay Miner. 41:280–287.

Laird, D.A., and R.H. Dowdy. 1994. Simultaneous quantification and chemical characterization of soil clays. Clays Clay Miner. 42: 747–754.

Laird, D.A., D.A. Martens, and W.L. Kingery. 2001. Nature of clay-humic complexes in an agricultural soil: I. Chemical, biochemical, and spectroscopic analyses. Soil Sci. Soc. Am. J. 65:1413–1418. (this issue)

Lal, R., J.M. Kimble, R.F. Follett, and B.A. Stewart (ed.) 1997. Management of carbon sequestration in soils. CRC Press, Boca Raton, FL.

Oades, J.M. 1988. The retention of organic matter in soils. Biogeochemistry 5:35–80.

Oades, J.M. 1989. An introduction to organic matter in mineral soils. p. 89–159. In J.B. Dixon and S.B. Weed (ed.) Minerals in soil environments. 2nd ed. SSSA, Madison, WI.

Schnitzer, M. 1986. Binding of humic substances by soil mineral colloids. p. 77–101. In P.M. Huang and M. Schnitzer (ed.) Interactions of soil minerals with natural organics and microbes. SSSA Spec. Publ. 17. SSSA, Madison, WI.

Stevenson, F.J. 1994. Humus chemistry. 2nd ed. John Wiley & Sons, New York.

United Nations. 1997. Koyoto Protocols to the United Nations framework convention on climate change. English Conference of the parties third session Koyoto, 1–10 Dec. 1997. available online at http://www.unfcc.int/resource/convkp.html (verified 27 Apr. 2001).

Wu, J., D.A. Laird, and M.L. Thompson. 1999. Sorption and desorption of copper on soil clay components. J. Environ. Qual. 28:334–338.